BACHELOR

The influence of the magnetic orientations on the exchange bias of a Pt/Co/IrMn system

Schippers, C.F.

Award date:
2015

The influence of the magnetic orientations on the exchange bias of a Pt/Co/IrMn system

C.F. Schippers

Supervisors:
ir. A. van den Brink
prof. dr. ir. H.J.M. Swagten

Tuesday 9th June, 2015

Abstract

In this report the influence of the magnetic orientations of the ferromagnetic layer and the anti-ferromagnetic layer in an exchange biased Pt/Co/IrMn system is determined. The magnetization of the samples was measured as a function of an external applied magnetic field. This measurement was done using an MPMS VSM-SQUID. From this magnetization the exchange bias and the coercivity could be determined.

The main result of these measurements was that the exchange bias was found to be independent of the magnetic orientations of the ferromagnetic layer and the anti-ferromagnetic layer. Results of a simulation using the Meiklejohn-Bean model agree with this experimental result, although the actual magnitudes of the exchange biases found in the simulation were slightly higher since the simulation does not account for domain formation. These experimental results and the simulation results are in contradiction to results found in literature, which state that the exchange bias depends on the magnetic orientations in the sample. The difference between the results of the experiments and the results found in literature could be caused by the fact that the literature concerns different exchange biased systems than the one used in this report.

Aside from the exchange bias, annealing a sample in a direction perpendicular to the direction of the ferromagnetic anisotropy was found to result in a reduced coercivity and a more gradual reversal of the magnetization. This can be explained by the fact that, for such a system, the exchange bias pull the magnetization somewhat out of the anisotropy direction, thereby lowering the energy needed to switch the magnetization.

Another interesting result is that annealing an in-plane ferromagnetic anisotropy sample in the out-of-plane direction did not result in an out-of-plane exchange bias. This may be caused by relaxation of the spins of the anti-ferromagnet into an in-plane direction after the annealing process. More research into this matter is needed.

The influence of the magnetic orientations on the exchange bias and the coercivity can be of interest for new magnetic sensors as well as for research into switching of magnetization without the application of external magnetic field.

Contents

Chapter 1

Introduction

Nowadays, in many systems magnetic sensors can be found. These sensors are being used for a wide variety of measurements, such as proximity and velocity. In tunnelling magneto resistance (TMR) and giant magneto resistance (GMR) sensors, the magnetic field can be determined by measuring the resistance of the sensor. The resistance is affected by the magnetic orientation of a free magnetic layer relative to the magnetic orientation of a fixed magnetic layer. Since the magnetic orientation of the free layer depends on the external magnetic field, the resistance of the sensor is related to te magnetic field.

This fixed magnetic layer can be made out of a ferromagnetic layer in combination with an anti-ferromagnetic layer. On the interface between the two layers, exchange coupling between the magnetic moments of both layers occurs. This exchange coupling causes an effective field on the ferromagnetic layer, which stabilizes the magnetization of the ferromagnetic layer. This effect is known as exchange bias and the effective field is the exchange bias field.

Traditionally both the ferromagnetic layer and the anti-ferromagnetic layer have an in-plane magnetic orientation, which causes the exchange bias to be in-plane as well. Experiments suggest that the magnitude of the exchange bias is dependent on the magnetic orientation of both the ferromagnetic layer and the anti-ferromagnetic layer (Maat, Takano, Parkin, & Fullerton, 2001; Sun, Zhou, Searson, & Chien, 2003). In this report the influences of the magnetic orientations of the ferromagnetic layer and the anti-ferromagnetic layer on the magnitude of the exchange bias are determined for a Pt/Co/IrMn system. In this system cobalt functions as the ferromagnet and iridium-manganese functions as the anti-ferromagnet. The platinum layer functions as a perpendicular magnetic anisotropy source. The influence of the magnetic orientations on the exchange bias can be of interest for new magnetic sensors as well as for research into switching of magnetization without the application of external magnetic field.

In the experiments for this report, four samples will be used. Two of the samples will have an in-plane ferromagnetic anisotropy, one with an in-plane and one with an out-of-plane anti-ferromagnetic magnetic orientation. The other two samples will have an out-of-plane ferromagnetic anisotropy, one with an in-plane and one with an out-of-plane anti-ferromagnetic magnetic orientation. The exchange bias of these samples will be measured using a VSM-SQUID and will be compared to each other and to a simulation of the samples using the Meiklejohn-Bean model.

In this report, first the theory behind exchange bias will be discussed. This will be done using the Meiklejohn-Bean model. Then the experimental set-up will be discussed. Finally, the results of the experiments and simulations are presented and discussed.

Chapter 2

Theory

In this chapter a brief introduction into ferromagnetism and anti-ferromagnetism is given, the theory behind exchange bias is discussed, in a phenomenological way and by using the Meiklejohn-Bean model, and a literature research on perpendicular exchange bias is presented. Also the thermal annealing process is treated.

2.1 Ferromagnetism and anti-ferromagnetism

Both ferromagnetism and anti-ferromagnetism are effects of exchange interaction between atoms that bear uncompensated electron spins. The energy E of exchange interaction between atoms i and j with spins $\mathbf{S}_i$ and $\mathbf{S}_j$, respectively, is given by (Kittel, 2005):

$$E = -2J_{EX}\mathbf{S}_i \cdot \mathbf{S}_j.$$

Here J_{EX} is the so called exchange integral. Since the exchange interaction is a short range interaction, one can assume that $J_{EX} \neq 0$ for neighbour spins and $J_{EX} = 0$ for other spins. When $J_{EX} > 0$ for neighbour spins, it is energetically favourable for the spins to align parallel to each other, resulting in a ferromagnet. When $J_{EX} < 0$ for neighbour spins, it is energetically favourable for the spins to align anti-parallel, resulting in an anti-ferromagnet.

Although the exchange interaction causes the spins to align parallel or anti-parallel, it does not introduce a preferred direction, or anisotropy, to which the spins align. For this report, the most interesting types of anisotropy are the magneto-crystalline anisotropy and the shape anisotropy. In magneto-crystalline anisotropy the crystallographic structure introduces one or more easy-axes. In shape-anisotropy, easy-axes are introduced by the shape of the material since the demagnetizing field is not equal for all directions.

2.2 Exchange Bias

In a system with a ferromagnetic (F) layer and an anti-ferromagnetic (AF) layer, such as shown in figure 2.1a, exchange coupling occurs between the spins on the interface between the F layer and the AF layer causing an exchange bias (EB). This exchange bias functions as an effective magnetic field in the system, which changes the magnitude of the external applied magnetic field that is needed to change the direction of the magnetization of the F layer. This results in a shift in the hysteresis curve of the magnetization of the F layer, measured as a function of the external applied magnetic field, as shown in figure 2.1b. The width of this hysteresis curve is twice the coercive field, H_C.

2.2.1 Meiklejohn-Bean model

One way to describe the exchange bias in a system which consists out of an F layer and an AF layer is by means of the ideal Meiklejohn-Bean model, which is based on the Stoner-Wohlfarth model for the

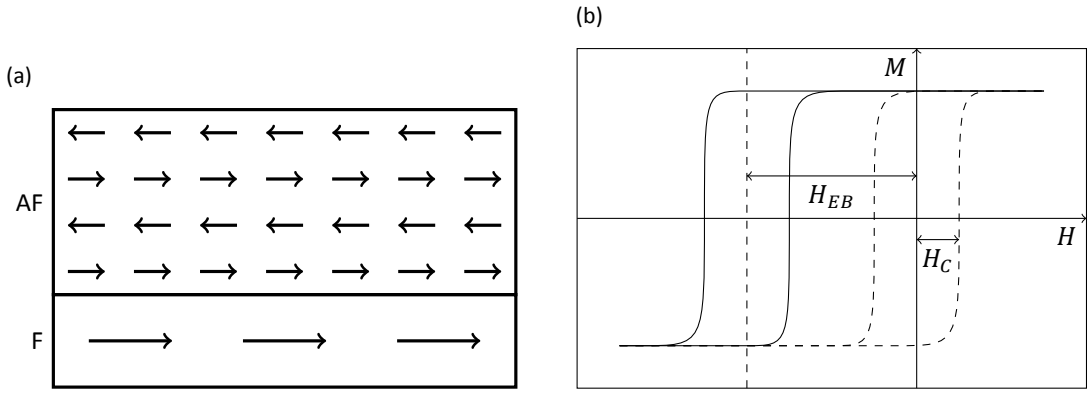

Figure 2.1: (a) A schematic view of a bilayer with an F layer with a in-plane magnetization and an AF layer with an in-plane magnetic orientation. (b) An example of a hysteresis curve of the magnetization as a function of the magnetic field. The dashed curve is without exchange bias, the solid curve is with exchange bias.

magnetization of an F layer. In this model, a number of assumptions are made (Radu & Zabel, 2008):

1. The F layer rotates rigidly, as a whole; all the magnetic moments of the F layer rotate in the same way.
2. The AF layer has an in-plane uni-axial anisotropy; it is energetically favourable for the AF layer that the spins in the AF align to the positive or negative direction of an easy-axis.
3. The spins on the interface of the AF layer are fully uncompensated; the interface of the AF has a net magnetization.
4. The AF layer is magnetically rigid; the spins in the AF layer always remain unchanged.
5. Both the F layer and the AF layer are in a single domain state; the layers are not divided into magnetic domains and thus the magnetic orientation is the the same over the entire layer.
6. The interface between the F layer and the AF layer is atomically smooth.
7. The F layer and the AF layer are coupled by an exchange interaction across the interface between the layers; J_{EB} is the inter-facial exchange coupling energy per unit area.

Within these assumptions the energy per area E_{A} of the system is given by (Radu & Zabel, 2008):

$$E_{\mathrm{A}} = -\mu_0 H M_{\mathrm{F}} t_{\mathrm{F}} \cos(\theta - \beta) + K_{\mathrm{F}} t_{\mathrm{F}} \sin^2(\beta) - J_{\mathrm{EB}} \cos(\beta), \tag{2.1}$$

In this formula, μ_0 is the vacuum permeability, M_{F}, t_{F} and K_{F} are the magnitude of the magnetization, the thickness and the anisotropy of the F layer, respectively, H is the magnitude of the external magnetic field and θ and β are the angles between the in-plane axis and the external magnetic field and between the in-plane axis and the magnetization direction of the F layer. These angles are depicted in figure 2.2a. The first term in the equation is caused by the Zeeman effect, this represents the interaction between the externally applied magnetic field and the magnetization of the F layer. The second term is caused by the anisotropy of the F layer. The last term is caused by the exchange interaction on the interface between the AF layer and the F layer.

In the more realistic version of this model, the fourth assumption, concerning the magnetic rigidity, is dropped and the AF layer is allowed to rotate slightly. This introduces a new variable α: the angle between the in-plane axis and the magnetic orientation of the AF layer. This angle is depicted in figure 2.2a. The addition of this new variable causes some changes to the energy function, which now becomes (Radu & Zabel, 2008):

$$E_{\mathrm{A}} = -\mu_0 H M_{\mathrm{F}} t_{\mathrm{F}} \cos(\theta - \beta) + K_{\mathrm{F}} t_{\mathrm{F}} \sin^2(\beta) + K_{\mathrm{AF}} t_{\mathrm{AF}} \sin^2(\alpha) - J_{\mathrm{EB}} \cos(\beta - \alpha), \tag{2.2}$$

in which K_{AF} and t_{AF} are the anisotropy and the thickness of the AF layer. The extra term is caused by the anisotropy of the AF layer. For the system used in the experiments in this report, the magnitude of K_{AF} is typical 10 times the magnitude of K_F for a rotation in the plane orthogonal to the sample.

With this Meiklejohn-Bean model, a simulation of a simplified F/AF bilayer can be done. In the simulation the directions of the magnetization of the ferromagnet, β, and the magnetic orientation of the anti-ferromagnet, α, are determined by minimizing the energy function of the model, equation (2.2), for these two variables. From these angles, which are measured with respect to the in-plane easy-axis, the easy-axis and hard-axis components can be calculated using the sine and the cosine, respectively. These components were calculated for each magnetic field in a full sweep. This full sweep is done twice, the first of which is in order to suppress artefacts caused by initial conditions, the second is for the actual results.

Besides using a simulation to determine the exchange bias it is also possible to derive an analytical solution for some systems by minimizing the energy for α and β. Therefore $\frac{\partial E_A}{\partial \beta}$ and $\frac{\partial E_A}{\partial \alpha}$ are set equal to 0 to find the minima or maxima of the energy:

$$\frac{H}{H_{EB}^{\infty}} \sin(\theta - \beta) + \frac{K_F}{H_{EB}^{\infty} \mu_0 M_F} \sin(2\beta) + \sin(\beta - \alpha) = 0, \tag{2.3a}$$

$$R \sin(2\alpha) - \sin(\beta - \alpha) = 0. \tag{2.3b}$$

Here the value of the EB field for an infinitely large AF anisotropy H_{EB}^{∞} and the ratio R between AF anisotropy energy and the inter-facial exchange energy are given by:

$$H_{EB}^{\infty} = -\frac{J_{EB}}{\mu_0 M_F t_F}, \tag{2.4a}$$

$$R = \frac{K_{AF} t_{AF}}{J_{EB}}. \tag{2.4b}$$

When neglecting the anisotropy of the F layer, so $K_F = 0$, and assuming $R \geq 1$, the EB field can be found by solving equations (2.3) for H using $\beta = \theta + \frac{\pi}{2}$. This results in:

$$H_{EB}(\theta) = H_{EB}^{\infty} \cos(\alpha_0 - \theta), \tag{2.5a}$$

$$= -\frac{J_{EB}}{\mu_0 M_F t_F} \cos(\alpha_0 - \theta), \tag{2.5b}$$

in which α_0 is the value for direction of the AF layer spins α at $\beta = \theta - \frac{\pi}{2}$. For situations where $R \gg 1$, which means that the AF anisotropy is very large and $\alpha \to 0$, the H_{EB} for an in-plane AF magnetic orientation is given by:

$$H_{EB}(\theta) = -\frac{J_{EB}}{\mu_0 M_F t_F} \cos(\theta). \tag{2.6}$$

Analogously, when $R \leq -1$ and $\alpha \to \frac{\pi}{2}$, H_{EB} for an out-of-plane AF magnetic orientation is given by

$$H_{EB}(\theta) = -\frac{J_{EB}}{\mu_0 M_F t_F} \sin(\theta). \tag{2.7}$$

This equations can be used to verify the simulation results.

2.3 Annealing

When a bilayer is deposited, the magnetic moments of the AF layer are not nicely ordered as in figure 2.1a, but are somewhat disordered. In order to align the magnetic moments in the AF layer, a thermal annealing process is used. During this process, the bilayer is heated to a temperature which is higher than the Néel temperature T_N of the AF layer, above which the AF material is not anti-ferromagnetic and the magnetic

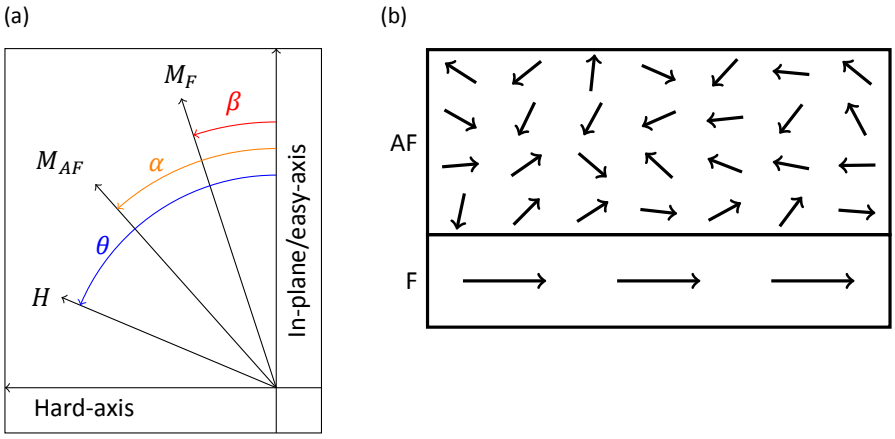

Figure 2.2: (a) An illustration of the angles used in the Meiklejohn-Bean model. (b) A schematic view of a bilayer with a temperature above the Néel temperature with an F layer with an in-plane magnetization and a disordered AF layer.

moments are fully disordered due to the high thermal energy of the spins, as can be seen in figure 2.2b. The temperature needs to be below the Curie temperature T_C above which the magnetization of the F layer vanishes, thus for the bilayer must hold $T_N < T_C$. At this temperature a field-cooling procedure is started: an external magnetic field is applied and the bilayer is cooled while the magnetic field is still applied, to a temperature below the Néel temperature. This causes the magnetic moments of the AF layer to align parallel or anti-parallel to the external applied magnetic field and thus results in the ordered magnetic orientation of the AF layer as shown in figure 2.1a.

2.4 Perpendicular exchange bias

In the bilayer shown in figure 2.1a, both the AF layer and the F layer have a parallel magnetic orientation, both in-plane, so the direction of the exchange bias is in-plane as well. A bilayer can also have other magnetic orientations in which the AF layer, the F layer, or both of the layers have an out-of-plane magnetic orientations. A lot of research is being done into systems in which the direction of the exchange bias is perpendicular to the sample plane, so called perpendicular exchange bias, since not only the direction of the exchange bias but also the magnitude depends on the magnetic orientation of the AF layer (Maat et al., 2001; Takahashi, Tsunoda, & Takahashi, 2012; Sun et al., 2003) although the mechanism behind the perpendicular exchange bias appears to be the same as responsible for the longitudinal exchange bias (Takahashi et al., 2012).

According to a study by Maat et al. (2001), using Co/Pt multi-layers, systems in which the AF layer was annealed in an out-of-plane direction have a smaller exchange bias compared to systems in which the AF layer was annealed in an in-plane direction. Their explanation for this observation is the fact that during the field cooling the spins will not freeze into a direction which is parallel to the field cooling direction, but into directions that are close to the field cooling direction and yield a lower energy due to magneto-crystalline anisotropy.

In an AF like iridium-manganese (IrMn) the spins are not simply horizontally or vertically aligned. The direction to which the spins align depends on the crystallographic structure of IrMn (Kohn et al., 2013). In figure 2.3a schematic view of the magnetic spin structure of a primitive cell of IrMn is shown. At each atomic site, the local spin can align parallel or anti-parallel to the depicted arrow. Two dimensional projections of the spin structure annealed in the horizontal direction and in the vertical direction are shown in figures 2.3b and 2.3c.

Since the exchange bias is caused by the spins on the interface between the F and AF layer, the direction and magnitude of the exchange bias is caused by the net magnetic moment of these surface spins. This causes a difference in magnitude of the exchange bias between in-plane and out-of-plane annealed samples. Since the samples used in the experiments are not single crystalline, the crystallographic structure will have different orientations in different parts of the sample, therefore the effect will be levelled and thus overestimated if one would try and calculate the exchange bias field using this spin structure.

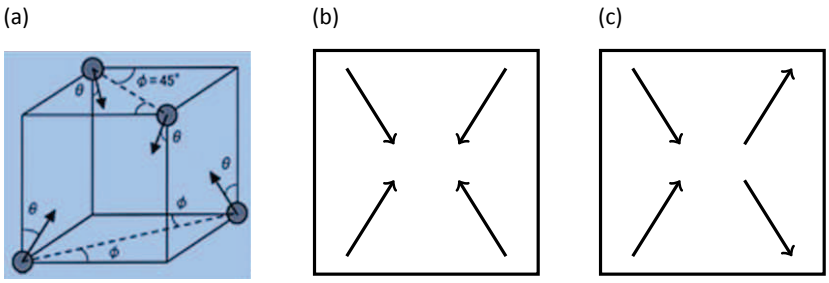

Figure 2.3: (a) The three dimensional spin structure of an IrMn cell. Adapted from Kohn et al. (2013). (b) & (c) Two dimensional projection of the spin structure of an IrMn cell in annealed in a (b) vertical and (c) horizontal direction.

A study by Sun et al. (2003) confirms that the out-of-plane exchange bias is smaller than the in-plane exchange bias. They found that in their FeMn/$[$FeNi/FeMn$]_4$ multilayer samples, the size of the out-of-plane exchange bias is about 85% of the in-plane exchange bias.

Chapter 3

Experimental set-up

In this chapter the experimental methods and the devices used in these experiments will be discussed as well as the samples used in the experiments. Also the MPMS VSM-SQUID is discussed.

3.1 Samples

In the samples used in the experiments for this report a Co film was used as F layer and an $Ir_{20}Mn_{80}$ film was used as AF layer. The samples were sputtered on top of a SiO_2 wafer in the CARUSO DC magnetron sputtering device. A schematic view of the samples is shown in figure 3.1. In these samples the magnetization of the F layer is dependent on the thickness of the Co layer. This is caused by the ratio between the perpendicular magnetic anisotropy (PMA) caused by the Pt layer underneath the Co layer, which introduces an easy axis in the out-of-plane direction, and the shape anisotropy, which introduces an easy axis in the in-plane direction. A thin Co layer results in an out-of-plane anisotropy since the PMA is dominant. A thick Co layer results in an in-plane magnetization since the shape anisotropy is dominant. For the out-of-plane magnetization the Co layer a thickness of 1.25 nm was used, while for the in-plane magnetization the Co layer a thickness of 5 nm was used.

The magnetic orientation of the AF layer is set by a thermal annealing process as described in section 2.3 in a MPMS VSM-SQUID. The thermal annealing process was done at a temperature of $500\ \mathrm{K}$ and a magnetic field of $2\ \mathrm{T}$. When the sample was heated and the magnetic field was applied, a delay of $1800\ \mathrm{s}$ was set before starting the field cooling. A set of four samples was made, so that there was one sample for each combination of out-of-plane or in-plane magnetization of the F layer with out-of-plane or in-plane magnetic orientation of the AF layer. A schematic view of the magnetic configurations of the set of four samples is shown in figure 3.2.

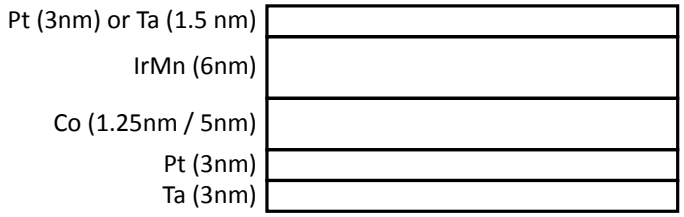

Figure 3.1: The schematic view of the samples used in the experiments for this report. The sample consists out of a layer of tantalum, platinum, cobalt, iridium-manganese and another layer of platinum or tantalum.

The magnetization of the samples was measured using the VSM-SQUID as a function of an external applied magnetic field. The magnetic field is decreased from a maximum field to a minimum field and then increased back to a maximum field. From these measurements the magnetic properties are extracted. The

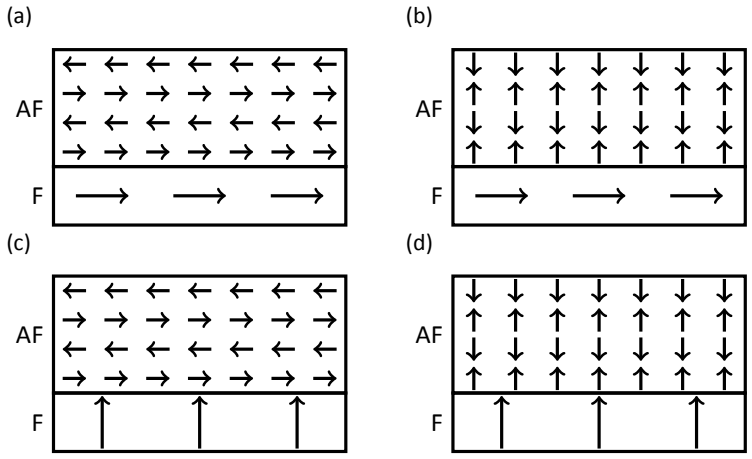

Figure 3.2: Schematic view of the magnetic configuration of the four samples. (a) In-plane F layer with in-plane AF layer. (b) In-plane F layer with out-of-plane AF layer. (c) Out-of-plane F layer with in-plane AF layer. (d) Out-of-plane F layer with out-of-plane AF layer.

exchange bias is determined by looking at the horizontal displacement of the hysteresis loop. The coercivity is determined by looking at the width of the hysteresis loop.

3.2 MPMS VSM-SQUID

A Quantum Design MPMS VSM-SQUID is used to anneal the samples and measure the magnetization of the samples. This MPMS (Magnetic Property Measurement System) combines the the ability of a VSM (Vibrating Sample Magnetometer) to measure the magnetization of a sample with the high accuracy of a DC SQUID (Superconducting Quantum Interferometer Device). The set of four pick-up coils in the MPMS VSM-SQUID are configured as a second-order gradiometer in order to increase the sensitivity by not measuring uniform magnetic fields and linear magnetic field gradients (Quantum Design, 2010). This results in a accuracy in the measured magnetic moment of up to $1 \times 10^{-8}\,\mathrm{emu} = 1 \times 10^{-12}\,\mathrm{A\,m^2}$. The MPMS VSM-SQUID used for the experiments in this report is equipped with an oven module, so it can reach temperatures ranging from $1.8\,\mathrm{K}$ to $1000\,\mathrm{K}$ (Quantum Design, n.d.).

In the VSM the sample is placed between the pick-up coils in a uniform magnetic field. A schematic view of the VSM is shown in figure 3.3a. The sample is then vibrated sinusoidally. If the sample has a net magnetization the vibration of the sample causes the magnetic flux through the pick-up coils to change sinusoidally. This induces a current in the the pick-up coils. The magnitude of this current is proportional to the magnetization of the sample.

The DC SQUID uses a two parallel placed Josephson junctions that separate two superconducting regions of a superconducting loop, as shown in figure 3.3b. Due to these Josephson junctions, the loop is only superconducting when the total current I is below a critical current I_C as can be seen in the I-V curve in figure 3.4. The SQUID makes use of the fact that within a superconducting loop the magnetic flux is quantized in magnetic flux quanta Φ_0 (Fagaly, 2006). When a magnetic flux Φ is applied through the loop, a screening current I_S in induced in order to keep the magnetic flux a integer multiple of the flux quantum Φ_0. A bias current I_B is applied that is slightly higher than the critical current I_C. Depending on the magnetic flux Φ, this screening current I_S will either increase or decrease the total current I. So changing the magnetic flux Φ will cause an oscillation in the measured voltage, in which each period corresponds to a change in the magnetic flux Φ of one magnetic flux quantum Φ_0, as shown in figure 3.4 (Fagaly, 2006). So by monitoring the changes in the measured voltage the magnetic flux Φ can be measured very accurately.

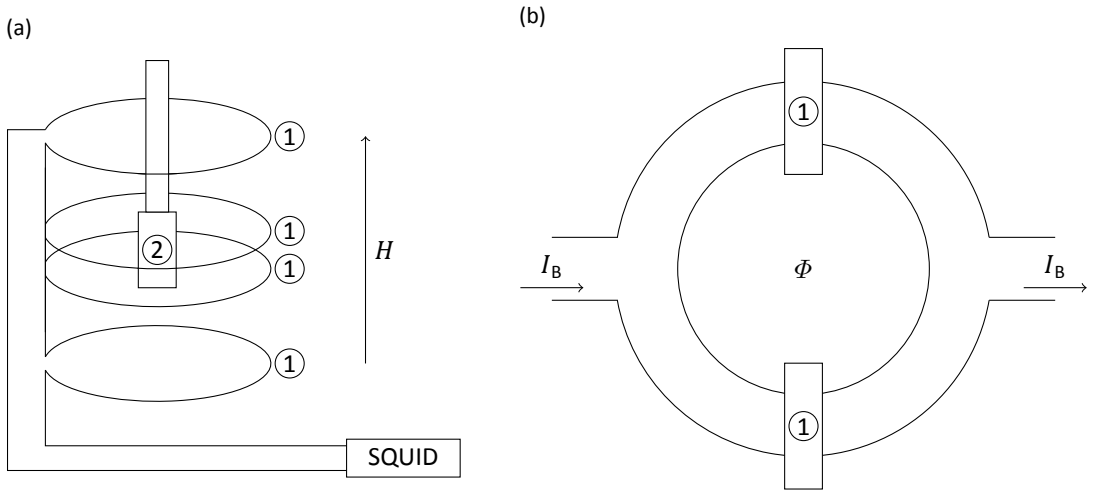

Figure 3.3: (a) schematic view from the VSM with superconducting pick-up coils, marked with ①, and a sample-holder on a sample-stick, marked with ②. The sample is oscillated parallel to the magnetic field direction. (b) Schematic view from the SQUID superconducting loop with two Josephson junctions marked with ①.

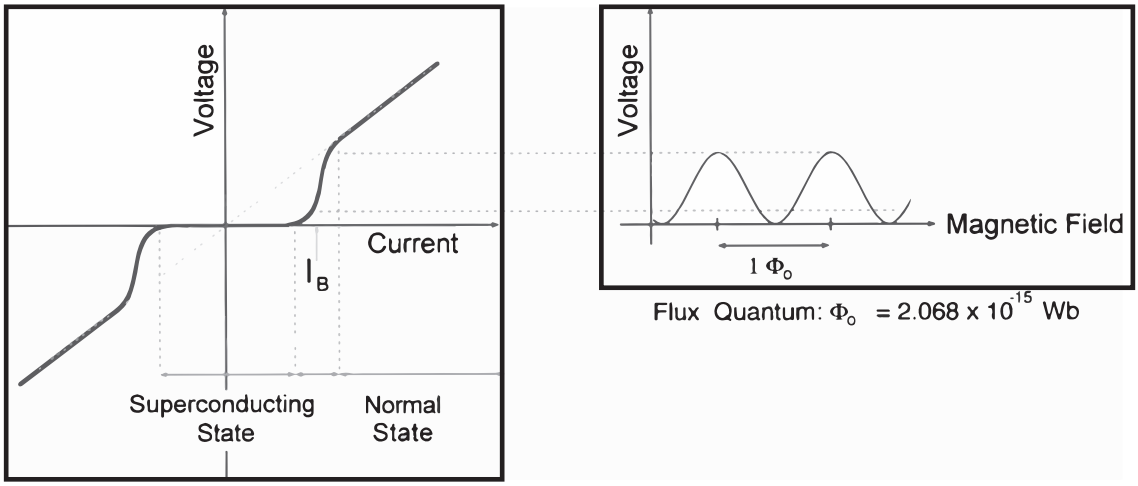

Figure 3.4: Left: I-V curve of the superconducting loop with two Josephson junctions. Right: voltage - magnetic flux curve for a constant bias current I_B. Adapted from Fagaly (2006).

When using the MPMS VSM-SQUID, the width of the sample is fixed to a maximum, the width of the sample holder, namely $5\ \mathrm{mm}$. The optimal length of the sample is $5\ \mathrm{mm}$; when the sample is shorter, there is less magnetic moment to measure, when the sample is longer, the change in magnetic flux will decrease. A downside of using the MPMS VSM-SQUID to anneal the sample is the fact that the sample holder that has to be used in te over module is made for measuring and annealing in the in-plane direction. When a sample is to be annealed in the out-of-plane direction, it has to be perpendicular attached to the sample holder. Therefore the sample is attached to the sample holder less firmly and not entirely perpendicular, causing an increased uncertainty in the annealing direction with respect to the sample.

Chapter 4

Results and discussion

In this chapter, the results of both the simulation and the experiments are presented and discussed. First the simulation of the Meiklejohn-Bean model is discussed. The used parameters are discussed, some energy-landscapes are presented and the results are presented, explained and compared to the literature.

Secondly, the experiments are discussed. The results of the measurements are presented, some observations are made, an attempt to explain these observations is made and the found exchange biases are discussed and compared to both literature and simulation results.

4.1 Simulation of the Meiklejohn-Bean model

The simulation was done for all four systems. For each system both an in-plane loop and an out-of-plane loop were simulated. The magnetization direction of F layer and magnetic orientation of the AF layer are determined by the sign of the F and AF anisotropy parameters K_{F} and K_{AF}, respectively; a positive anisotropy results in an in-plane direction, while a negative anisotropy results in an out-of-plane direction. Moreover, the magnetization of a sample with an in-plane F anisotropy measured along the in-plane easy-axis is likely to rotate through the in-plane hard-axis rather than through the out-of-plane hard-axis, since the F anisotropy for this rotation is lower than for an out-of-plane rotation. In order to compare the results of the simulation to the results of the experiments, the thickness of the F layer is also changed when changing it's anisotropy, since the direction of the anisotropy in the real samples is determined by the thickness. The effective ferromagnetic anisotropy for rotations through the out-of-plane is set to $K_{\mathrm{F}} = 1 \times 10^5\,\mathrm{Jm}^{-3}$, based on the order of magnitude found using (Pizzini et al., 2014):

$$B_0 = \frac{2K_{\mathrm{F}}}{M_{\mathrm{F}}}, \tag{4.1}$$

in which B_0 is the magnetic field needed to reach the in-plane saturation magnetization M_{F} for an F layer with an out-of-plane anisotropy, or vice versa. The values for $B_0 = 0.5\,\mathrm{T}$ and $M_{\mathrm{F}} = 1 \times 10^6\,\mathrm{Am}^{-1}$ are based upon values found in the experiments. The effective ferromagnetic anisotropy for rotations through the in-plane hard-axis is set to $K_{\mathrm{F}} = 0.05 \times 10^5\,\mathrm{Jm}^{-3}$, which is chosen to get results of which the coercivity corresponds to the coercivity found during experiments. $J_{\mathrm{EB}} = 1 \times 10^{-4}\,\mathrm{Jm}^{-2}$ and $K_{\mathrm{AF}} = 1 \times 10^6\,\mathrm{Jm}^{-3}$ are based upon values found in studies by Nicolodi et al. (2012) and Aley et al. (2009), respectively.

In figure 4.1, a couple of energy landscapes are displayed for several external magnetic field magnitudes for both an in-plane and an out-of-plane AF magnetic orientation, both with an in-plane F anisotropy. For each of the external magnetic fields, the local minimum, starting from the local minimum of the preceding magnetic field, is determined. By plotting the found local minima as a function of the magnetic field, the magnetizations curves are found, as shown in figures in figures 4.2 and 4.3.

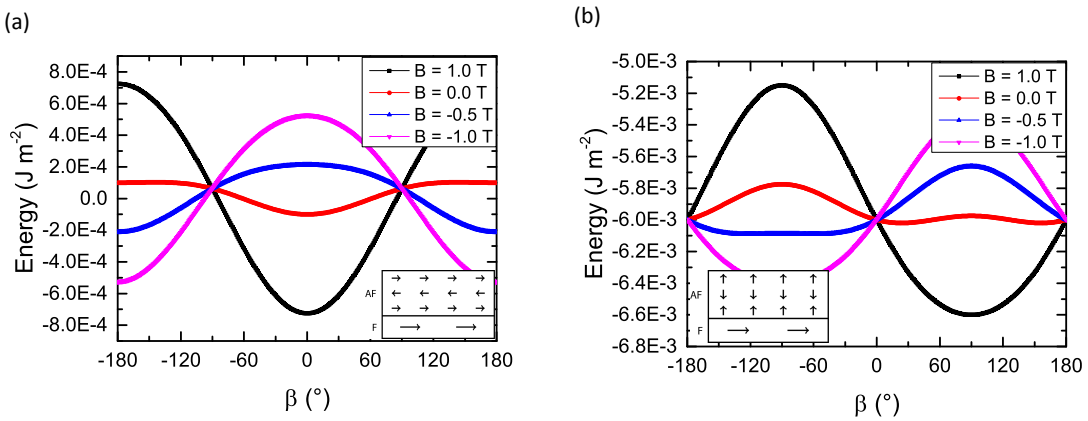

Figure 4.1: Energy landscapes for an in-plane anisotropy of the F layer (a) with an in-plane and (b) with an out-of-plane magnetic orientation in the AF layer as a function of the magnetization angle β. For each AF anisotropy, several landscapes for varying external applied magnetic fields, parallel to the magnetic orientation of the AF layer, are shown.

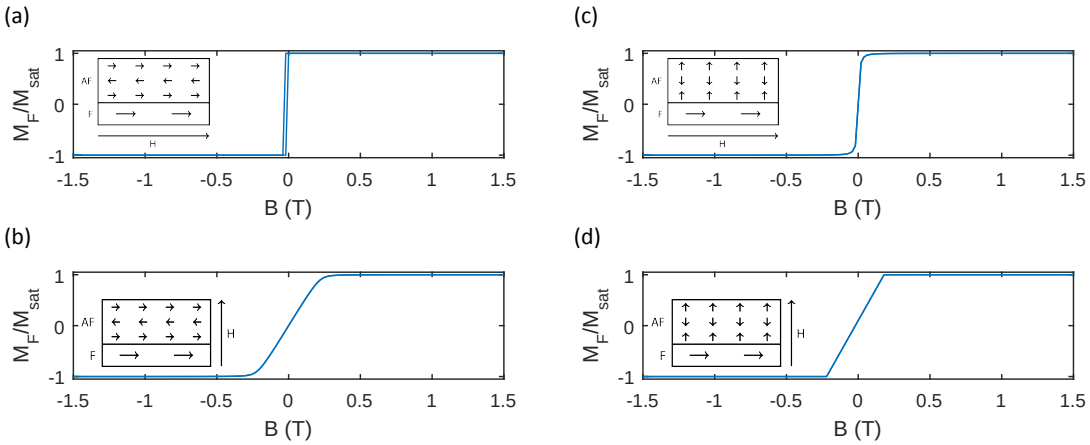

Figure 4.2: Simulation results for systems in which the F layer has an in-plane magnetic orientation. In figures (a) and (b), the AF layer has an in-plane magnetic orientation. Along the in-plane easy-axis (a) $B_{\mathrm{EB}} = 18.7\,\mathrm{mT}$ and $B_{\mathrm{C}} = 9.37\,\mathrm{mT}$ is found. Along the out-of-plane axis (b) $B_{\mathrm{EB}} = 2.75 \times 10^{-3}\,\mathrm{mT}$ and $B_{\mathrm{C}} = 3.55 \times 10^{-4}\,\mathrm{mT}$ is found. In figures (c) and (d) the AF layer has an out-of-plane magnetic orientation. Along the in-plane easy-axis (c) $B_{\mathrm{EB}} = 3.29 \times 10^{-4}\,\mathrm{mT}$ and $B_{\mathrm{C}} = 4.59 \times 10^{-5}\,\mathrm{mT}$ is found. Along the out-of-plane axis (d) $B_{\mathrm{EB}} = 20.0\,\mathrm{mT}$ and $B_{\mathrm{C}} = 5.02 \times 10^{-3}\,\mathrm{mT}$ is found.

4.1.1 Exchange bias

The exchange biases for the situations in which the magnetic field is perpendicular to the magnetic orientation of the AF layer are in the range of 10^{-6} through 10^{-7}. These small exchange biasses may be caused by numerical errors, since the exchange bias in the direction perpendicular to the magnetic orientation of the AF layer should vanish.

The exchange biases for the situations in which the magnetic field direction is parallel to the magnetic orientation of the AF layer are larger. These values are shown in table 4.1. The found exchange bias magnitudes for the systems with an out-of-plane F anisotropy are the same for the in-plane and the out-of-plane AF magnetic orientation. Also, the magnitudes of the exchange biases for the systems with an in-plane F anisotropy are the same for the in-plane and the out-of-plane AF magnetic orientation.

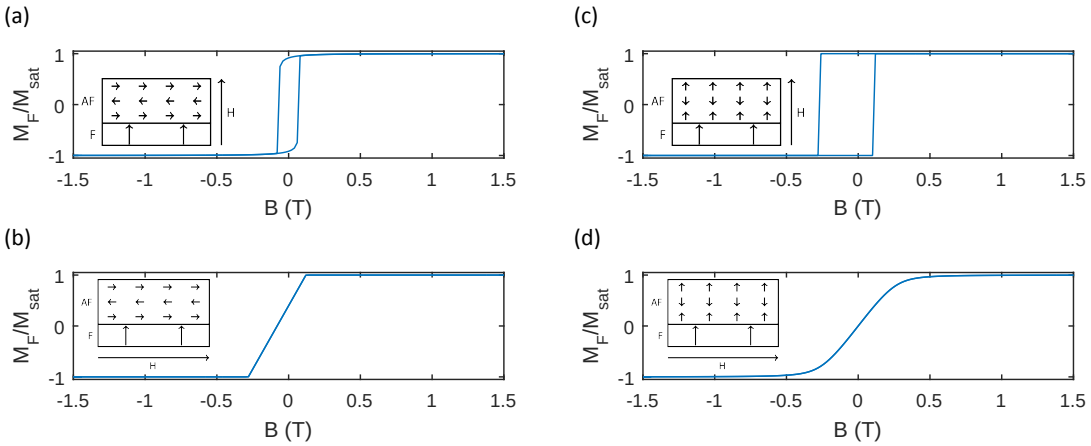

Figure 4.3: Simulation results for systems in which the F layer has an out-of-plane magnetic orientation. In figures (a) and (b), the AF layer has an in-plane magnetic orientation. Along the out-of-plane axis (a) $B_{EB} = 5.49 \times 10^{-4}\,\mathrm{mT}$ and $B_C = 66.9\,\mathrm{mT}$ is found. Along the in-plane axis (b) $B_{EB} = 80.0\,\mathrm{mT}$ and $B_C = 2.11 \times 10^{-3}\,\mathrm{mT}$ is found. In figures (c) and (d) the AF layer has an out-of-plane magnetic orientation. Along the out-of-axis (c) $B_{EB} = 80.1\,\mathrm{mT}$ and $B_C = 190\,\mathrm{mT}$ is found. Along the in-plane axis (d) $B_{EB} = 4.02 \times 10^{-3}\,\mathrm{mT}$ and $B_C = 6.83 \times 10^{-6}\,\mathrm{mT}$ is found.

Table 4.1: Exchange biases from simulations for systems in which the direction of the magnetic field is parallel to the magnetic orientation of the AF layer. All values, except for the in-plane F layer with the in-plane AF layer, are consistent with the result of equations 2.6 and 2.7.

	In-plane F layer	Out-of-plane F layer
In-plane AF layer	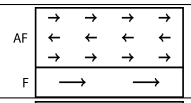 18.7 mT	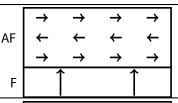 80.0 mT
Out-of-plane AF layer	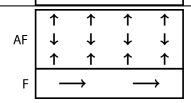 20.0 mT	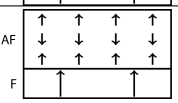 80.1 mT

Moreover, one can see that the exchange bias for the out-of-plane anisotropy of the F layer is larger compared to the in-plane F layer. This is due to the fact that the out-of-plane F layer is thinner compared to the in-plane F layer in order to get it out-of-plane and thus the exchange interaction energy term is relatively more important. From equations (2.6) and (2.7), one can expect the relation $B_{EB} \propto \frac{1}{t_F}$. This relation is consistent with the values shown in table 4.1, except for the system with the in-plane AF layer because the value of K_F used for this system is different from the value used for the others systems as explained before. The use of a different values for K_F causes some fluctuations in the exchange bias, although this is more likely to be a numerical artefact than a physical phenomenon.

The exchange biases found in the simulation are in contradiction with literature, which states that the exchange bias for systems with an out-of-plane field cooling direction and thus an out-of-plane magnetic orientation for the AF layer is smaller than for systems with an in-plane field cooling direction. The difference between the results of the simulation and the literature can be caused by the fact that the Meiklejohn-Bean model is a simplified model and doesn't include the spin structures of the F or AF layer, three dimensional rotation, domain formation etcetera.

Table 4.2: Coercivities from simulations for systems in which the direction of the magnetic field is parallel to the F anisotropy.

	In-plane F layer	Out-of-plane F layer
In-plane AF layer	9.37 mT	66.9 mT
Out-of-plane AF layer	4.59×10^{-5} mT	190 mT

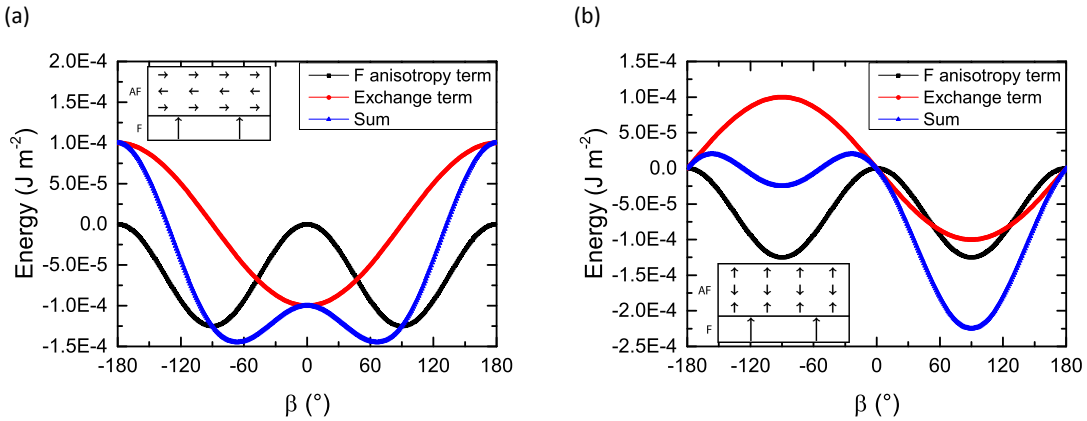

Figure 4.4: Separate terms of the energy landscapes for an out-of-plane anisotropy of the F layer (a) with an in-plane and (b) with an out-of-plane magnetic orientation in the AF layer as a function of the magnetization angle β. In both graphs the F anisotropy energy, the exchange energy and the sum of those two energies are displayed.

4.1.2 Coercivity

One can notice that the AF magnetic orientation also influences the coercivity of the systems. In general, coercivity is only expected when the magnetic field direction is parallel to the F anisotropy direction. This holds for the simulations since the coercivities found for systems in which the magnetic field direction is perpendicular to the F anisotropy direction are in the range of 10^{-6} to 10^{-9}. The coercivities of the remaining systems are shown in table 4.2. In this table, one can see that the coercivity is larger for systems in which the AF magnetic orientation and the F anisotropy are co-linear. This can be explained by looking at the energy landscapes shown in figure 4.4, in which one can see that the barrier around $\beta = 0°$ in the F anisotropy term, that causes the coercivity, is decreased by the exchange term if the F anisotropy and AF magnetic orientation are perpendicular. If the F anisotropy and AF magnetic orientation are co-linear, the exchange energy effectively just shifts the barrier of the F anisotropy term. Moreover, the coercivity in the systems with an in-plane F anisotropy is lower than systems with an out-of-plane F anisotropy. This is caused by the fact that both in-plane F anisotropy systems have a lower K_F value than the out-of-plane F anisotropy systems, as explained before.

4.1.3 Rounding

The magnetization curves of systems in which the magnetic field direction is perpendicular to the AF anisotropy show rounded corners, whereas magnetization curves of systems in which the magnetic field direction is parallel to the AF anisotropy show straight corners. This can be explained by taking into account the effective magnetic field on the F layer. This effective magnetic field is the sum of the exchange bias field and the external magnetic field. When the AF anisotropy, and thus the exchange bias field, is perpendicular

to the external magnetic field, the direction of the effective magnetic field is canted and therefore it will not pull the F magnetization in either the in-plane of out-of-plane direction, but rather in a direction that is somewhere in between those two direction. Since the graphs show either the in-plane or out-of-plane component of the magnetization, this will result in rounded corners.

4.2 Experiments

After the annealing process, the magnetic moment of the samples is measured using the VSM-SQUID. In order to avoid any influence of the training effect two hysteresis loops were measured and were compared to each other. The magnetic moment measured by the VSM-SQUID is given in $\mathrm{erg G^{-1}} = 10^{-3}\,\mathrm{Am^2}$. This value is divided by the volume of the Co layer of the sample and is corrected for the linear diamagnetic response of the sample holder. The slope of this linear response is determined by linear fits through both ends of the measurements. The saturation magnetizations of the samples is somewhat lower than the value saturation magnetization for pure cobalt, $M_S = 1.4 \times 10^6\,\mathrm{Am^{-1}}$ (Machlin, 2010). This may be due to the fact that only a thin Co layer is used in these samples. The results are presented in figures 4.5 through 4.10. Measurements of the samples before the annealing process are shown in appendix A.

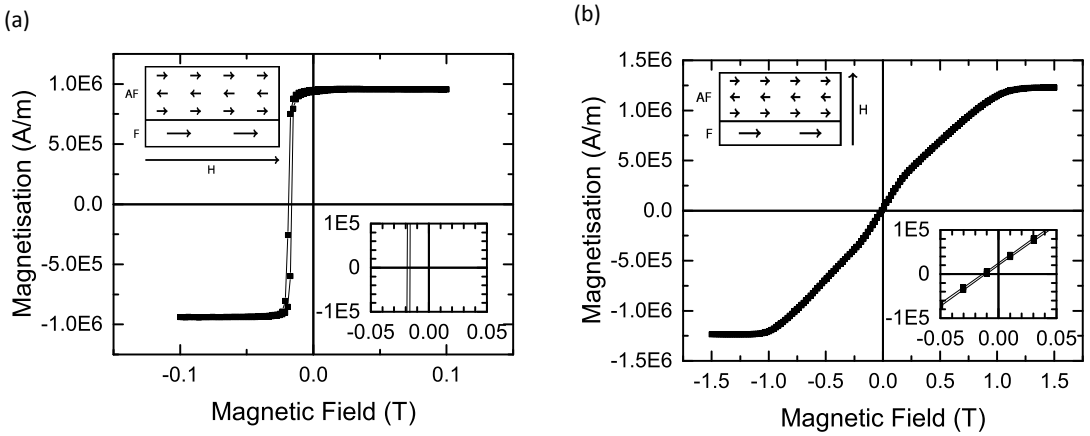

Figure 4.5: Magnetization of a sample with an in-plane F anisotropy and an in-plane AF field cooling direction measured along (a) the in-plane direction ($B_{\mathrm{EB}} = 17.5\,\mathrm{mT}$ and $B_{\mathrm{C}} = 1.17\,\mathrm{mT}$) and (b) the out-of-plane direction ($B_{\mathrm{EB}} = 12.2\,\mathrm{mT}$ and $B_{\mathrm{C}} = 1.41\,\mathrm{mT}$). In the out-of-plane measurement, the slope around zero is slightly increased. This may be explained by the existence of grains with a different anisotropy, although additional research is necessary. The unexpected exchange bias in the out-of-plane direction may be an artefact of the measurement or may be caused by an additional anisotropy source, although more research is needed.

4.2.1 Exchange bias

An overview of the measured exchange biases in the field-cooling direction is found in table 4.3. The exchange bias of the out-of-plane annealed in-plane F anisotropy sample is very large compared to the other found exchange biases where it is expected to have a similar or smaller magnitude of exchange bias compared to the other exchange biases according to the simulations, as shown in section 4.1.1, and literature, as presented in section 2.4, respectively. This large out-of-plane exchange bias may be explained by the fact that the sample is not positioned exactly orthogonal to the sample holder, as described in section 3.2, but rather with an estimated offset of 5° in the angle between the sample plane and the sample holder. Due to this offset in the angle and the strong in-plane F anisotropy, the magnetization of the F layer switches from one in-plane direction into another rather than into an out-of-plane direction. Therefore, the measured exchange bias is the in-plane exchange bias but, since only the in-plane component of the

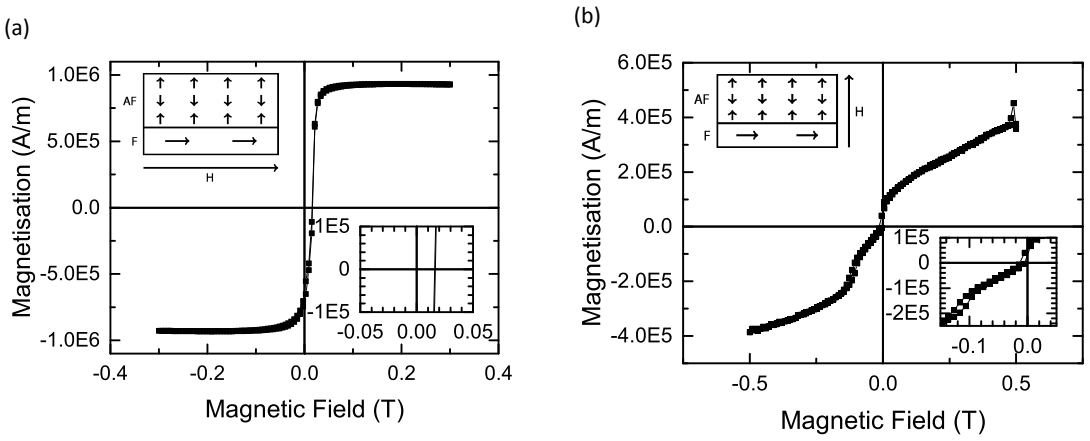

Figure 4.6: Magnetization of a sample with an in-plane F anisotropy and an out-of-plane AF field cooling direction measured along (a) the in-plane direction ($B_{\mathrm{EB}} = 16.3\,\mathrm{mT}$ and $B_{\mathrm{C}} = 0.274\,\mathrm{mT}$) and (b) the out-of-plane direction ($B_{\mathrm{EB}} = 111\,\mathrm{mT}$ and $B_{\mathrm{C}} = 5.05\,\mathrm{mT}$). The out-of-plane measurement is not corrected for a diamagnetic background signal, since the slope of the correction could not be determined due to the fact that the saturation magnetization is not reached. The in-plane measurement shows an unexpected exchange bias, which could be caused by an unsuccessful annealing process in the out-of-plane direction. The additional jump in magnetization around zero magnetic field found in the out-of-plane measurement could be explained by inhomogeneous heating during the annealing process. The large exchange bias in the out-of-plane direction could be caused by an offset in the angle between the sample plane and the sample holder. The perturbation at the right end of the out-of-plane measurement can be given appears to be an artefact in the measurement and can therefore be neglected.

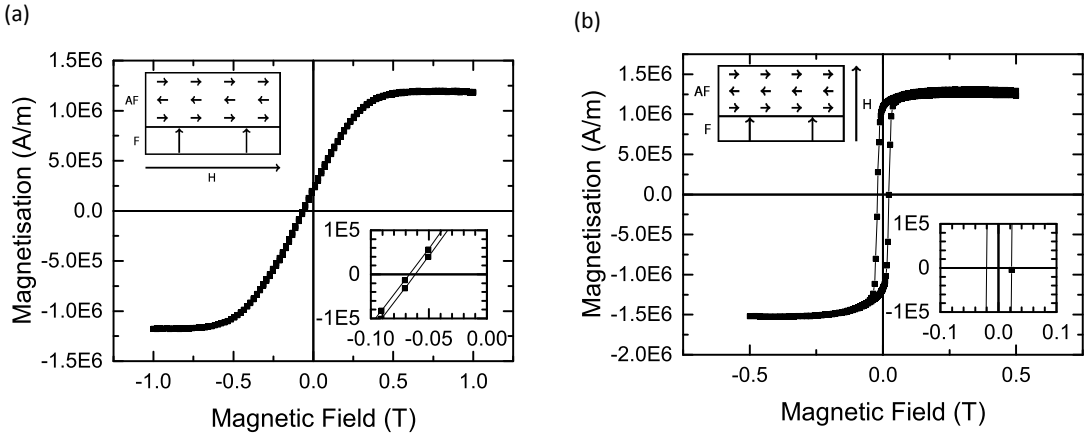

Figure 4.7: Magnetization of a sample with an out-of-plane F anisotropy and an in-plane AF field cooling direction measured along (a) the in-plane direction ($B_{\mathrm{EB}} = 66.3\,\mathrm{mT}$ and $B_{\mathrm{C}} = 2.66\,\mathrm{mT}$) and (b) the out-of-plane direction ($B_{\mathrm{EB}} = 0.342\,\mathrm{mT}$ and $B_{\mathrm{C}} = 22.7\,\mathrm{mT}$). The in-plane measurement shows an unexpected coercivity.

magnetic field can switch the direction of the magnetization, it appears to be significantly larger.

When looking at the in-plane annealed samples, one could notice that the exchange biases of the sample with an out-of-plane F anisotropy is 3.79 times the exchange bias of the sample with an in-plane F anisotropy. This can be explained by the fact that the thickness of the F layer of the in-plane F anisotropy samples is 4 times the thickness of the F layer of the out-of-plane anisotropy samples. Therefore, since the exchange bias is an interface effect, it has four times as much influence in the out-of-plane F anisotropy samples

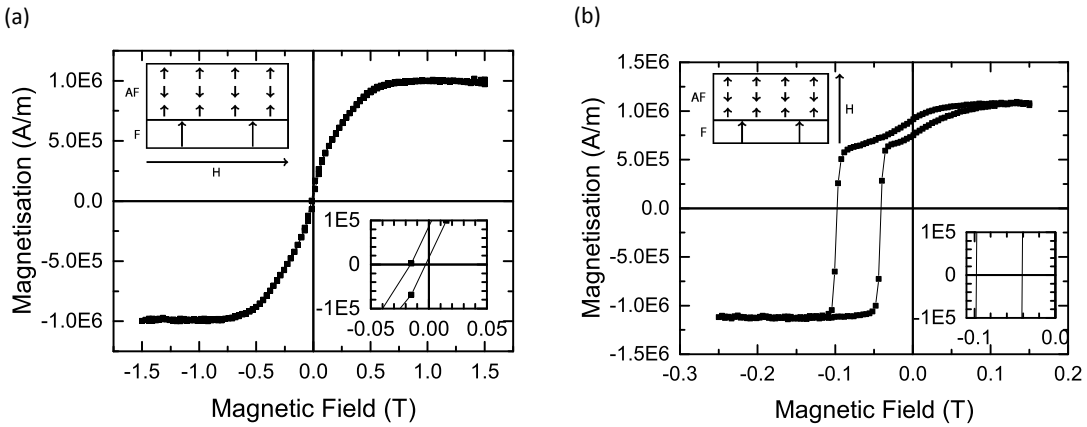

Figure 4.8: Magnetization of a sample with an out-of-plane F anisotropy and an out-of-plane AF field cooling direction measured along (a) the in-plane direction ($B_{\mathrm{EB}} = 9.39\,\mathrm{mT}$ and $B_{\mathrm{C}} = 6.61\,\mathrm{mT}$) and (b) the out-of-plane direction ($B_{\mathrm{EB}} = 69.4\,\mathrm{mT}$ and $B_{\mathrm{C}} = 28.3\,\mathrm{mT}$). In the in-plane measurement, the slope around zero magnetic field is slightly increased which may be due to the existence of grains with a different anisotropy. The in-plane measurement also shows an unexpected exchange bias and coercivity. The unexpected exchange bias could be an artefact of the fact that the sample was not exactly orthogonal during the annealing. In the out-of-plane measurement, a small hysteresis can be seen around zero magnetic field. This could be caused by an inhomogeneous temperature distribution during the annealing process.

Table 4.3: Overview of the exchange biases measured along the field-cooling direction.

	In-plane F layer	Out-of-plane F layer
In-plane AF layer	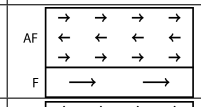 17.5 mT	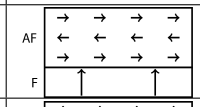 66.3 mT
Out-of-plane AF layer	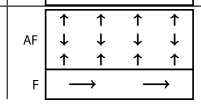 111 mT	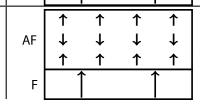 69.4 mT

compared to the in-plane F anisotropy samples. This observation is consistent both with the simulations and equations (2.6) and (2.7).

The exchange biases of the samples with an out-of-plane F anisotropy are of the same order of magnitude, although the out-of-plane exchange bias is slightly higher. This is consistent with the results found in the simulations. However, the result of both the experiments and the results are in contradiction with the results discussed in literature (Maat et al., 2001; Sun et al., 2003). This could be due to the fact that the results in literature concern different exchange biased systems than the system used in the experiments in this report.

The measured exchange biases in the direction perpendicular to the field-cooling direction are shown in table 4.4. Since the exchange bias direction is expected to be parallel to the field-cooling direction, these exchange biases are expected to vanish. The exchange biases in the out-of-plane direction of the in-plane annealed out-of-plane F anisotropy sample is small and can be considered negligible.

The exchange bias in the in-plane direction of the out-of-plane annealed out-of-plane F anisotropy sample is larger but can be explained by the fact that the sample was not positioned exactly orthogonal to the sample holder, as stated in section 3.2. An uncertainty of 5° was estimated for the angle between the sample plane and the sample holder. This caused the field-cooling direction to be not exactly out-of-plane, but slightly canted to the in-plane direction. The direction of the exchange bias is then slightly canted to

the in-plane direction and therefore a small in-plane component of the exchange bias is measured. The in-plane exchange bias of the out-of-plane annealed in-plane F anisotropy sample may be caused by the fact that the AF spins relax into an in-plane orientation within the spin structure of IrMn. This would also explain the fact that, besides the exchange bias of $111\ \mathrm{mT}$, no out-of-plane exchange bias was found in this sample after out-of-plane annealing. More research is needed into this matter.

The exchange bias measured along the out-of-plane direction of the in-plane annealed in-plane F anisotropy sample is the same order of magnitude as the exchange bias measured along the in-plane direction of this sample. This unexpected exchange bias may be an artefact of the measurement, but since no convenient explanation could be found, more research into this matter is necessary. More insight on this result could be offered by measuring the magnetization of the sample while rotating a magnetic field with a constant magnitude.

Table 4.4: Overview of the exchange biases measured in the direction perpendicular to the field-cooling direction.

	In-plane F layer	Out-of-plane F layer
In-plane AF layer	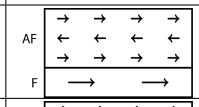 12.2 mT	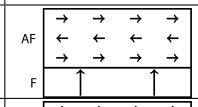 0.342 mT
Out-of-plane AF layer	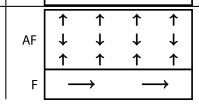 16.3 mT	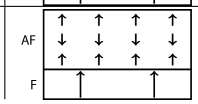 9.39 mT

4.2.2 Coercivity

The measured coercivities in the direction of the F anisotropy are presented in table 4.5. The coercivities of samples with an out-of-plane F layer are relatively high compared to the coercivities of sample with an in-plane sample. This is caused by the fact that the magnetization of the in-plane F anisotropy sample is able to rotate in the sample plane without having to rotate through the out-of-plane direction, which would take more magnetic field to achieve, while the magnetization of the out-of-plane F anisotropy sample has to rotate through the in-plane direction.

Table 4.5: Overview of the coercivities measured along the F anisotropy direction.

	In-plane F layer	Out-of-plane F layer
In-plane AF layer	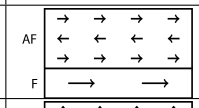 1.17 mT	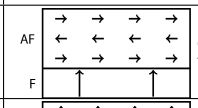 22.7 mT
Out-of-plane AF layer	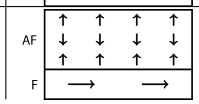 0.274 mT	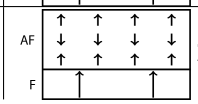 28.3 mT

Moreover the samples in which the field-cooling direction is co-linear with the F anisotropy direction have a higher coercivity than the samples in which those two directions are perpendicular. This is due to the fact that for systems in which the two directions are perpendicular, the exchange bias already pulls the magnetization of the F layer a little bit out of the F anisotropy direction, thereby lowering the energy needed for the magnetization to switch direction. This result agrees with the results of the simulations, although the actual values and differences between values may be lower than in the simulations since switching may happen by domain formation instead of through rotation of the entire magnetization, which is not taken into account in the simulation.

The coercivities measured along the direction perpendicular to the F anisotropy are presented in table 4.6, although these coercivities were expected to vanish. This could be causes by the presence of less stable grains in the AF layer. These less stable grains could have enough thermal energy at room temperature to overcome the energy barrier that keeps the spins aligned to the spin structure of IrMn. This decreases the exchange bias since the magnetic moments of these grains are able to rotate together with the F layer. Since the magnetic moment of such a grain at the surface between the F layer and the AF layer is still exchange coupled to the magnetic moments of the F layer, it takes more energy to switch the magnetization in either direction, thereby causing an increased coercivity.

Table 4.6: Overview of the coercivities measured in the direction perpendicular to the F anisotropy.

	In-plane F layer	Out-of-plane F layer
In-plane AF layer	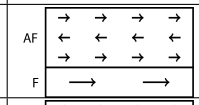 $1.41\,\mathrm{mT}$	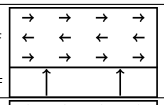 $2.66\,\mathrm{mT}$
Out-of-plane AF layer	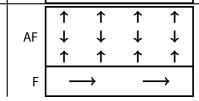 $5.05\,\mathrm{mT}$	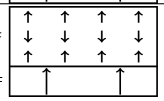 $6.61\,\mathrm{mT}$

4.2.3 Rounding

Every measurement shows some degree of rounding in the magnetization around the switching, whereas in the simulations only the systems in which the AF magnetic orientation was perpendicular to the magnetic field direction. This could be caused by the existence of domains, which is not allowed in the Meiklejohn-Bean model. Some of the domains will switch more easily than others, especially if the magnetic field direction is perpendicular to the F anisotropy direction. Since this effect adds to the effect in which the effective field on the F layer is slightly canted due to the addition of the exchange bias field to the external magnetic field, as described in section 4.1.3, a stronger rounding can be found on measurements in which the field-cooling direction is perpendicular to the magnetic field direction.

4.2.4 Out-of-plane annealing

As one can see in figure 4.8b besides the hysteresis with an exchange bias of $69.4\,\mathrm{mT}$, a smaller hysteresis around $0\,\mathrm{T}$ is found in the out-of-plane annealed out-of-plane F anisotropy sample. This could be caused by the positioning during the out-of-plane annealing. Since the sample plane was perpendicular to the sample holder plane, only the side of the sample was directly attached to the sample holder with the heating module and the thermocouple. Therefore the sample could have had an inhomogeneous temperature distribution during the annealing process, leaving some regions that are not annealed.

Another measurement was done with a sample with an out-of-plane F anisotropy that was annealed in the out-of-plane direction in an Ar oven at $500\,\mathrm{K}$ and $200\,\mathrm{mT}$. This oven should provide a more homogeneous temperature distribution over the sample. The results of the measurements, measured with the MPMS VSM-SQUID, are shown in figure 4.9. The exchange bias found in the out-of-plane direction in this measurement $66.6\,\mathrm{mT}$. The switch around zero magnetic field in the previous measurement is significantly reduced. The remaining switch could be caused by some remaining silver-paste used during the annealing process in the Ar oven, causing a small paramagnetic signal.

The out-of-plane annealed in-plane F anisotropy sample, of which the measurements are presented in figure 4.6 shows this artefact as well and this can be explained by the same effect. Moreover, this sample shows some other artefacts. The out-of-plane exchange bias is very high, $111\,\mathrm{mT}$, compared to the in-plane annealed exchange bias of the in-plane sample, while, according to both literature, as reported in section 2.4, and simulations, as seen in section 4.1.1, this should be the other way around.

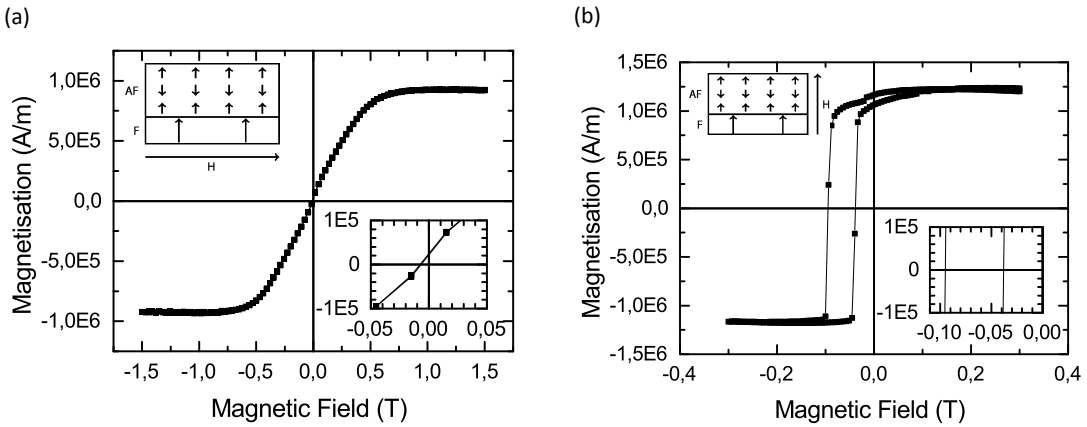

Figure 4.9: Magnetization of a sample with an out-of-plane F anisotropy and an out-of-plane AF field cooling direction in a $200\,\mathrm{mT}$ magnetic field measured along (a) the in-plane direction ($B_{\mathrm{EB}} = 7.13\,\mathrm{mT}$ and $B_{\mathrm{C}} = 0.435\,\mathrm{mT}$) and (b) the out-of-plane direction ($B_{\mathrm{EB}} = 66.7\,\mathrm{mT}$ and $B_{\mathrm{C}} = 27.3\,\mathrm{mT}$). This sample is similar to the sample used for the measurement shown in figure 4.8 but is annealed using the Ar oven in stead of using the MPMS VSM-SQUID. The measurement is done using the MPMS VSM-SQUID. In the in-plane measurement an unexpected exchange bias is measured, which may be an artefact of the fact that the sample was not exactly orthogonal to the field-cooling direction during the annealing. In the out-of-plane measurement a small artefact in the magnetization can be seen, this may be caused by the paramagnetic response of the silver-paste that is used during the annealing process in the Ar oven.

This high exchange bias may be the result of an offset in the angle between the sample and the sample holder and is in fact a measurement of the in-plane exchange bias, as was more extensively explained in section 4.2.1. Besides this very strong exchange bias, no out-of-plane exchange bias was found in this sample.

Also, the in-plane measurements, presented in figure 4.5a, shows an in-plane exchange bias of $16.3\,\mathrm{mT}$, which is of the same order of magnitude as the in-plane exchange bias of the in-plane annealed in-plane F anisotropy sample. This may be explained by the fact that the AF spins relax to an in-plane orientation within the spin structure of IrMn after the annealing process, as stated in section 4.2.1. This would also explain the fact that, besides the $111\,\mathrm{mT}$ exchange bias, no out-of-plane exchange bias was found in this sample. More research into this matter is needed.

4.2.5 Increased slope around zero magnetic field

In the hard-axis loops that are shown in figures 4.5b, 4.8a and 4.10a, the slope of the magnetization curve is increased around zero magnetic field. This could be caused by the existence of grains that have a different anisotropy compared to the rest of the sample. This may be explained by an inhomogeneous temperature distribution during the annealing process, both for the out-of-plane annealed sample, as explained in section 4.2.4, and the in-plane annealed sample, due to the fact that the VSM-SQUID heats the sample using two spirals. Therefore the sample could have a higher temperature directly above one of the spirals, whereas the rest of the sample has a slightly lower temperature. This would explain why the in-plane measurement of the out-of-plane F anisotropy sample that was out-of-plane annealed in the Ar oven, as shown in figure 4.9a, does not show such an increased slope around zero magnetic field, in contrast to when this sample was out-of-plane annealed in the VSM-SQUID, as shown in figure 4.8a. More research into this matter is needed.

4.2.6 Degradation

Since the magnetic field range of the measurement as shown in figure 4.6b was not high enough for the sample to reach the saturation magnetization, another measurement with a higher magnetic field range was done with this sample. This measurement was done 17 days after the annealing process while the first measurement was done within one day after the annealing process. The measurement, as shown in figure 4.10a, shows virtually no exchange bias, $B_{\mathrm{EB}} = 0.294\,\mathrm{mT}$. This would be expected if the sample was indeed in-plane annealed as suggested in section 4.2.4.

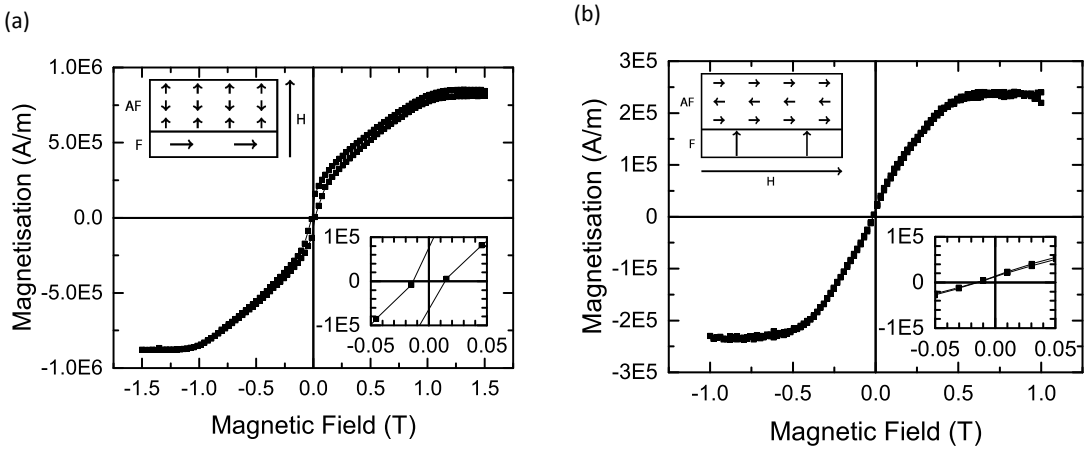

Figure 4.10: (a) Magnetization of a sample with an in-plane F anisotropy and an out-of-plane field cooling direction, measured along the out-of-plane direction, 17 days after the annealing process; $B_{\mathrm{EB}} = 0.294\,\mathrm{mT}$ and $B_{\mathrm{C}} = 13.8\,\mathrm{mT}$. The sample shows virtually no exchange bias, which may be explained by the fact that the AF spins relax to an in-plane orientation after the annealing process. The slope of the magnetization curve is slightly increased around zero magnetic field. This may be caused by the existence of grains with a different anisotropy, although more research into this matter is needed. (b) Magnetization of a sample with an out-of-plane F anisotropy and an in-plane field cooling direction, measured along the in-plane direction, 28 days after the annealing process; $B_{\mathrm{EB}} = 15.2\,\mathrm{mT}$ and $B_{\mathrm{C}} = 0.541\,\mathrm{mT}$. Due to degradation, the exchange bias is significantly less then during the measurement directly after annealing and the saturation magnetization is strongly reduced.

A second measurement of the out-of-plane F anisotropy sample that is annealed in the in-plane direction, corresponding to the measurement in figure 4.7a, was done 28 days after the annealing process. This measurement, presented in figure 4.10b, shows an exchange bias of $15.2\,\mathrm{mT}$, which is reduced from $66.3\,\mathrm{mT}$ in the earlier measurement. Also the saturation magnetization is reduced from $1.17 \times 10^6\,\mathrm{A \cdot m^{-1}}$ to $0.235 \times 10^6\,\mathrm{A \cdot m^{-1}}$. A possible explanation for this behaviour is that degradation in the samples takes place. This could be due to diffusion of Mn atoms from the AF layer through the entire sample (Takiguchi, Ishii, Makino, & Okabe, 2000).

Chapter 5

Conclusion

In this chapter the overview of the research done in this report is given. Also, an outlook for further research is given.

The aim of this report was to determine the influence of the magnetic orientations of the ferromagnetic layer and the anti-ferromagnetic layer on the exchange bias of a Pt/Co/IrMn system. The samples used for the experiment were grown in a DC sputtering magnetron. The samples were then annealed in an MPMS VSM-SQUID. After the annealing, the magnetization of the samples was measured using the MPMS VSM-SQUID. From the magnetization curves the exchange bias and the coercivity were extracted.

Then the measured exchange biases in the field-cooling directions of the four magnetic orientations were compared. The extremely large exchange bias found in the out-of-plane annealed sample with an in-plane F anisotropy is caused by the very strong in-plane anisotropy of the F layer, due to which the annealing was unsuccessful. Moreover, the exchange biases of the samples with an out-of-plane F anisotropy have an exchange bias that is slightly less than four times as large as the exchange bias found in the in-plane annealed sample with an in-plane F anisotropy. This is due to the fact that the exchange bias in the out-of-plane sample has relatively more influence on the magnetization of the F layer since the F layers of the in-plane F anisotropy samples are four times as thick as the F layers of the out-of-plane F anisotropy samples. This relation is consistent with both the theory and the simulation results.

The in-plane annealed in-plane F anisotropy sample, when multiplied by four in order to compensate for the layer thickness, has the same magnitude as the exchange biases of the out-of-plane F anisotropy samples. Therefore, no difference could be found between an in-plane or an out-of-plane exchange bias. This result is consistent with the results from the simulations, although the actual magnitudes of the exchange biases found in the simulations are higher. This can be explained by the fact that the model used in the simulation doesn't include domain formation, due to which the exchange biases are being overestimated in the simulations.

These results are in contradiction to the results found in literature, which states that the exchange bias for the out-of-plane annealed samples is lower than for the in-plane annealed samples. The difference between the results found in the experiments and the results as found in literature may be explained by the fact that the results discussed in literature concern different exchange biased systems than the one used in this report.

In the direction perpendicular to the field-cooling directions, unexpected exchange biases are found. The in-plane exchange biases found in the out-of-plane annealed out-of-plane F anisotropy samples can be explained by the fact that the sample was not positioned exactly orthogonal to the external magnetic field, due to which an in-plane exchange bias arises. The in-plane exchange bias in the out-of-plane annealed sample with an in-plane F anisotropy may be caused by the fact that the AF spins relax into an in-plane direction within the IrMn spin structure after the annealing process. More research into this matter is needed.

The out-of-plane exchange bias in the in-plane annealed sample with an in-plane F anisotropy may be an artefact of the measurement. Since no convenient explanation could be found, additional research into this matter is necessary. A measurement of the magnetization while a magnetic field with a constant magnitude is rotated through the in-plane directions could provide more insight in this result.

When the coercivities in the direction of the F anisotropy are compared, one can see that the in-plane F samples have a lower coercivity, due to the fact that the magnetization of these samples is able to rotate through the sample plane, while the out-of-plane sample needs to rotate through an in-plane direction. Moreover, the samples which are annealed in the direction of the F anisotropy have an higher coercivity then the samples which are annealed in the direction perpendicular to the F anisotropy. This is caused by the fact that, in the perpendicular situation, the exchange bias pulls the magnetization somewhat out of the F anisotropy direction, thereby lowering the energy needed to switch the magnetization direction. This effect also results in a more gradual magnetization reversal for the orthogonal systems.

Unexpected coercivities are found in the directions perpendicular to the F anisotropy direction, in which the coercivity is expected to vanish. This could be explained by the presence of less stable grains in the AF layer that have enough thermal energy at room temperature to overcome the barrier that keeps the spins aligned to the spin structure of IrMn. The magnetic moments of these can rotate together with the magnetic moments of the F layer but, since they are still exchange coupled to the spins of the F layer, it takes more energy to switch the magnetization in either direction, thereby causing an increased coercivity.

Another unexpected result is an increased slope around zero magnetic field in three of the hard-axis loops. This may be due to the existence of grains with a different anisotropy, which could be caused by an inhomogeneous temperature distribution during the annealing process. More research into this matter is needed.

More research on this matter is needed in order to fully understand the perpendicular exchange bias. It would be interesting to measure the exchange bias for a successful in-plane annealed sample.

Bibliography

Aley, N., Kroeger, R., Lafferty, B., Agnew, J., Lu, Y., & O'Grady, K. (2009, October). Tuning of Anisotropy in IrMn/CoFe Exchange Bias Systems. *IEEE Transactions on Magnetics*, *45*(10), 3869–3872. doi:10.1109/TMAG.2009.2024955

Fagaly, R. L. (2006, October). Superconducting quantum interference device instruments and applications. *Review of Scientific Instruments*, *77*(10), 101101. doi:10.1063/1.2354545

Kittel, C. (2005). *Introduction to solid state physics*. Wiley.

Kohn, A., Kovács, A., Fan, R., McIntyre, G. J., Ward, R. C. C., & Goff, J. P. (2013). The antiferromagnetic structures of IrMn3 and their influence on exchange-bias. *Scientific reports*, *3*, 2412. doi:10.1038/srep02412

Maat, S., Takano, K., Parkin, S. S. P., & Fullerton, E. E. (2001, August). Perpendicular Exchange Bias of Co / Pt Multilayers. *Physical Review Letters*, *87*(8), 087202. doi:10.1103/PhysRevLett.87.087202

Machlin, E. (2010). *Materials Science in Microelectronics II: The effects of structure on properties in thin films*. Elsevier.

Nicolodi, S., Pereira, L. G., Harres, A., Azevedo, G. M., Schmidt, J. E., Garcia-Aguilar, I., … Geshev, J. (2012, June). Negative rotatable anisotropy in IrMn/Cr/Co thin films. *Physical Review B*, *85*(22), 224438. doi:10.1103/PhysRevB.85.224438

Pizzini, S., Vogel, J., Rohart, S., Buda-Prejbeanu, L. D., Jué, E., Boulle, O., … Thiaville, A. (2014, July). Chirality-Induced Asymmetric Magnetic Nucleation in Pt / Co / AlO x Ultrathin Microstructures. *Physical Review Letters*, *113*(4), 047203. doi:10.1103/PhysRevLett.113.047203

Quantum Design. (n.d.). *MPMS® SQUID VSM Product Information*.

Quantum Design. (2010). Magnetic Property Measurement System SQUID VSM User's Manual.

Radu, F. & Zabel, H. (2008). Exchange bias effect of ferro-/ antiferromagnetic heterostructures. In H. Zabel & S. D. Bader (Eds.), *Magnetic heterostructures* (Vol. 227, pp. 97–184). Springer Tracts in Modern Physics. Berlin, Heidelberg: Springer. doi:10.1007/978-3-540-73462-8

Sun, L., Zhou, S. M., Searson, P. C., & Chien, C. L. (2003, May). Longitudinal and perpendicular exchange bias in FeMn/(FeNi/FeMn)n multilayers. *Journal of Applied Physics*, *93*(10), 6841. doi:10.1063/1.1544447

Takahashi, H., Tsunoda, M., & Takahashi, M. (2012, November). Perpendicular Exchange Anisotropy in Mn-Ir/Fe-Co/[Pt/Co]4 Multilayers. *IEEE Transactions on Magnetics*, *48*(11), 4347–4350. doi:10.1109/TMAG.2012.2196760

Takiguchi, M., Ishii, S., Makino, E., & Okabe, A. (2000, March). Thermal degradation of spin valve multilayers caused by Mn migration. *Journal of Applied Physics*, *87*(5), 2469. doi:10.1063/1.372204

Appendices

Appendix A

As deposited hysteresis loops

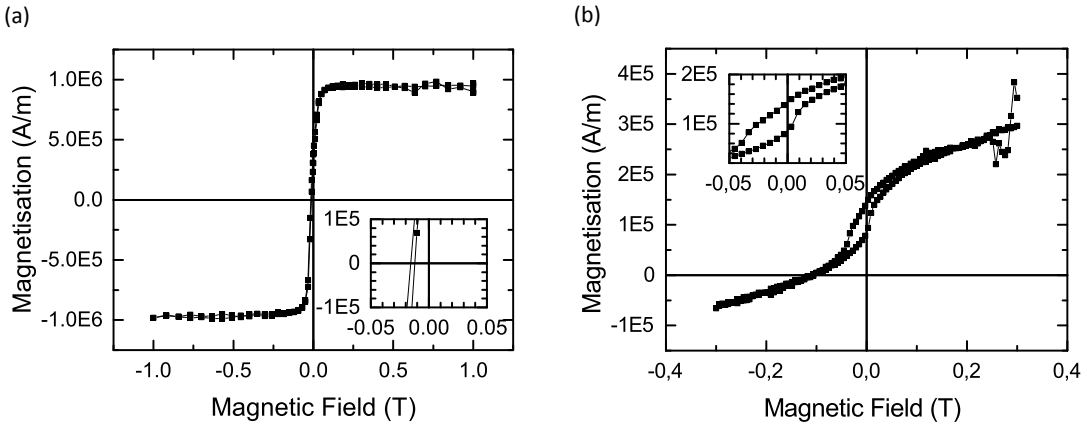

Figure A.1: As deposited loops of the sample with the in-plane F anisotropy, measured along the in-plane (a) and out-of-plane (b) axis. The out-of-plane measurement is not corrected for a linear background signal since the saturation magnetization is not reached and the linear correction could not be determined.

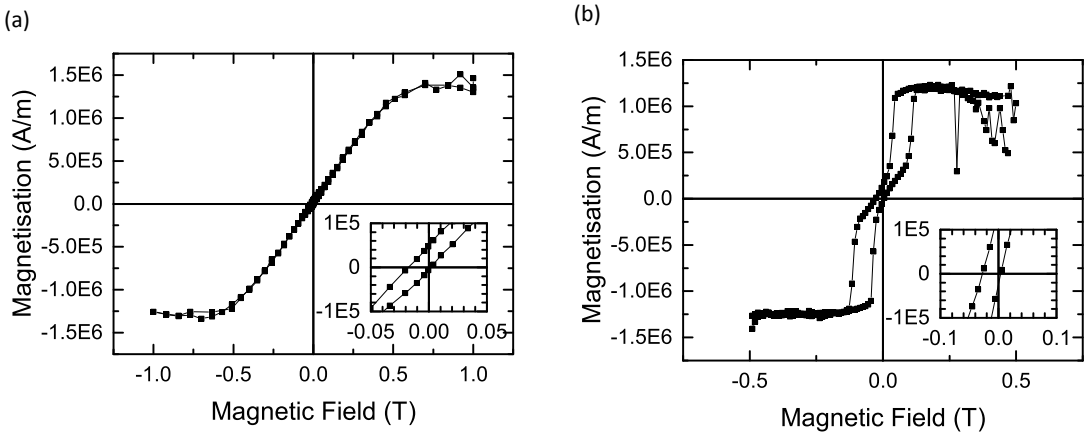

Figure A.2: As deposited loops of the sample with the out-of-plane F anisotropy, measured along the in-plane (a) and out-of-plane(b) axis.